



A Novel Pathway of Atmospheric Sulfate Formation Through Carbonate Radical

Yangyang Liu^{1,2}, Yue Deng^{1,2}, Jiarong Liu³, Xiaozhong Fang¹, Tao Wang¹, Kejian Li¹, Kedong Gong¹, Aziz U. Bacha¹, Iqra Nabi¹, Xiuhui Zhang³, Christian George⁴, and Liwu Zhang^{1,2}

5

¹Shanghai Key Laboratory of Atmospheric Particle Pollution and Prevention, Department of Environmental Science and Engineering, Fudan University, Shanghai, 200433, P. R. China.

²Shanghai Institute of Pollution Control and Ecological Security, Shanghai, 200092, Peoples' Republic of China.

³Key Laboratory of Cluster Science, Ministry of Education of China, School of Chemistry and Chemical Engineering, Beijing Institute of Technology, Beijing 100081, P. R. China

⁴Univ. Lyon, Université Claude Bernard Lyon 1, CNRS, IRCELYON, F-69626, Villeurbanne, France.

Correspondence to: Liwu Zhang (zhanglw@fudan.edu.cn)

Abstract. Carbon dioxide is considered an inert gas that rarely participates in atmospheric chemical reactions. However, we show here that CO₂ is involved in some important photo-oxidation reactions in the atmosphere through the formation of carbonate radicals (CO₃^{•-}). This potentially active intermediate CO₃^{•-} is routinely overlooked in atmospheric chemistry regarding its effect on sulfate formation. Present work demonstrates that SO₂ uptake coefficient is enhanced by 17 times on mineral dust particles driven by CO₃^{•-}. It can be produced through two routes over mineral dust surfaces: i) hydroxyl radical + CO₃²⁻; ii) holes (h⁺) + CO₃²⁻. Employing a suite of laboratory investigations of sulfate formation in the presence of carbonate radical on the model and authentic dust particles, field measurements of sulfate and (bi)carbonate ions within ambient PM, together with density functional theory (DFT) calculations for single electron transfer processes in terms of CO₃^{•-}-initiated S(IV) oxidation, a new role of carbonate radical in atmospheric chemistry is elucidated.

1. Introduction

Atmospheric composition changes are subjected to highly reactive light-induced radicals, such as hydroxyl (•OH), hydroperoxyl (HO₂•), or nitrate radicals (NO₃•), which are able to alter not only compositions but also physical and chemical properties of particulate matter (Thompson, 1992; Prinn et al., 2001; Platt et al., 1990; Davis and Francisco, 2011). However, when atmospheric chemical reactions occur over nanometer-sized particles at ambient condition, which creates a locally enriched aqueous medium of unique chemical activity, other radicals might likewise gain importance. The carbonate radical (CO₃^{•-}) is typically such an active radical. The lifetime of CO₃^{•-} ranges from a microsecond to even a few milliseconds and its concentration can be two orders of magnitude higher than that of hydroxyl radicals over the water surface (Chandrasekaran and Thomas, 1983; Goldstein et al., 2001; Shafirovich et al., 2001; Sulzberger et al., 1997a). In addition, the one-electron



reduction potential of $E^0(\text{CO}_3^{\cdot-}/\text{CO}_3^{2-})$ couple is 1.78 V vs. NHE at neutral pH, leaving $\text{CO}_3^{\cdot-}$ a strong oxidant in aquatic chemistry (Cope et al., 1973 ;Bisby et al., 1998;Merouani et al., 2010). Previous studies concerning carbonate radical in aqueous media demonstrate that it reacts rapidly with some organic compounds with higher selectivity (Merouani et al., 2010), especially for those electron-rich compounds amines (Stenman et al., 2003;Yan et al., 2019). Also, it has been pointed out that the scavenging of hydroxyl radicals by (bi)carbonate species leads to the formation of $\text{CO}_3^{\cdot-}$ ions (Graedel and Weschler, 1981b), which promotes the degradation of phenol (Xiong et al., 2016). Besides, a higher second order of rate constant, lying at $10^9 \text{ M}^{-1} \text{ s}^{-1}$, has been reported for the reaction of $\text{CO}_3^{\cdot-}$ with porphyrins (Ferrer-Sueta et al., 2003), indicating that this radical ion has great oxidation capability that may trigger atmospherically relevant chemical reactions. However, it is only regarded as an intermediate in tropospheric anion chemistry so far (Graedel and Weschler, 1981a;Dotan et al., 1977;Lehtipalo et al., 2016;Beig and Brasseur, 2000) and its underlying role as an active oxidant for heterogeneous reaction in the atmosphere is barely explored. Very recently, our group observed the promotional effect of $\text{CO}_3^{\cdot-}$ on atmospheric nitrate formation (Fang et al., 2021). Motivated by this finding, attempts were made to further explore its role in other important atmospherically-relevant reactions.

It is well documented that sulfate (SO_4^{2-}) is also a key constituent of aerosols in the atmosphere (Huang et al., 2015;Su et al., 2016). It is able to serve as the precursors of efficient cloud condensation nuclei, with optical properties leading to a cooling effect (Wang et al., 2011). As a consequence, the mechanism aspect of secondary sulfate formation was the focus of numerous studies over the past decades (Hung et al., 2018;Stone, 2002;Zhang et al., 2015b). There is a consensus that high-valence sulfur (VI), produced from the oxidation of anthropogenic SO_2 , is the dominant source for atmospheric secondary sulfate. However, a remarkable missing sulfate budget emerges for the atmospheric modeling, which underpredicts SO_4^{2-} by over 50 % (normalized mean bias) in comparison to observational results when heterogeneous aerosol chemistry is not considered (Zheng et al., 2015). This large gap indicates that there are unknown heterogeneous reaction pathways of significance and unconsidered promoters that have great potential to accelerate sulfate formation.

Due to the high stability of CO_2 under ambient conditions (Hossain et al., 2020), there are rare studies concerning the influence of CO_2 in atmospheric chemical processes. CO_2 is demonstrated to form (bi)carbonate species over humidified dust particles (Baltrusaitis et al., 2011;Nanayakkara et al., 2014) and reduced to CO under solar illumination (Deng et al., 2020). However, its impact on atmospheric heterogeneous reactions remains poorly characterized. Our recent laboratory study shows that CO_2 impacts the sulfate formation on aluminum oxide particles in the dark (Liu et al., 2020) while upon solar illumination its role in SO_2 oxidation over mineral dust surfaces is still an open question. Carbonate salt is enriched in authentic dust aerosol (Cao et al., 2005) and reported to reach over 10 % wt. of Asian dust particles (McNaughton et al., 2009). It is generally accepted that CO_3^{2-} affects atmospheric chemistry and aerosol characteristics mainly through its intrinsic alkalinity, which buffers aerosol acidity and favors the sulfate formation (Bao et al., 2010;Kerminen et al., 2001;Yu et al., 2018). In fact, either CO_2 or carbonate salt is able to produce the active $\text{CO}_3^{\cdot-}$ under the ambient circumstance and increase the oxidative capacity in the atmosphere. Combined with our earlier investigation of $\text{CO}_3^{\cdot-}$ (Fang et al., 2021), this



65 radical ion is likely to be a driving force for fast SO₂ oxidation. However, to the best of our knowledge, no work has considered how and to what extent the carbonate radical influences SO₂ heterogeneous oxidation in the atmosphere.

In the current study, through laboratory studies, we present that carbon dioxide and calcium carbonate, working as the precursor of carbonate radicals, extend their ability to accelerate sulfate formation over authentic particles in the atmosphere. Together with quantum chemistry calculations, a detailed molecular mechanism regarding a single electron transfer (SET)
70 process between carbonate radical and sulfite ions is elucidated. Furthermore, field observations validate findings from the laboratory investigations.

2. Experimental methods

2.1 Laboratory Studies

A series of characterizations were initially performed to investigate the mineral dust of concern by using X-ray diffraction
75 (XRD) and Raman. The heterogeneous reaction of SO₂ on mineral dust particles in the presence of CO₂ and carbonate species were then investigated by the *in situ* Fourier transform spectrum (DRIFTS), ion chromatography (IC), Raman, electron spin resonance (ESR), and nanosecond transient absorption spectroscopy (NTAS). Furthermore, we employed three types of authentic dust particles and four kinds of synthesized authentic simulants to probe the proposed scheme. All corresponding configuration setup, characterizations, and methodologies can be found in Supplement, text 1-12, Tables S1-
80 S3 and Fig. S1-S10. In terms of oxygen isotope experiments, more detailed procedures are available in Supplement, text 15.

2.2 Quantum Chemical Calculation

We employed density functional theory (DFT) calculations in the term of single electron transfer (SET) process using Gaussian 09 package to investigate this novel route, detailed in Supplement text 13-14 and Fig. S11-S12.

2.3 Field Observations

85 Atmospheric aerosols were collected on the roof of our department using an 8-stage non-viable-cascade-impactor type sampler (TISCH TE Inc., USA), with details shown in supplement Text 16. The concentration of water-soluble sulfate ion was by measured IC analysis while that of (bi)carbonate ions were determined by the ionization balance approach (Supplement, text 17 and 18). The relationship between (bi)carbonate ions and sulfate ions during the daytime and nighttime hours were then determined.



90 3. Results and discussion

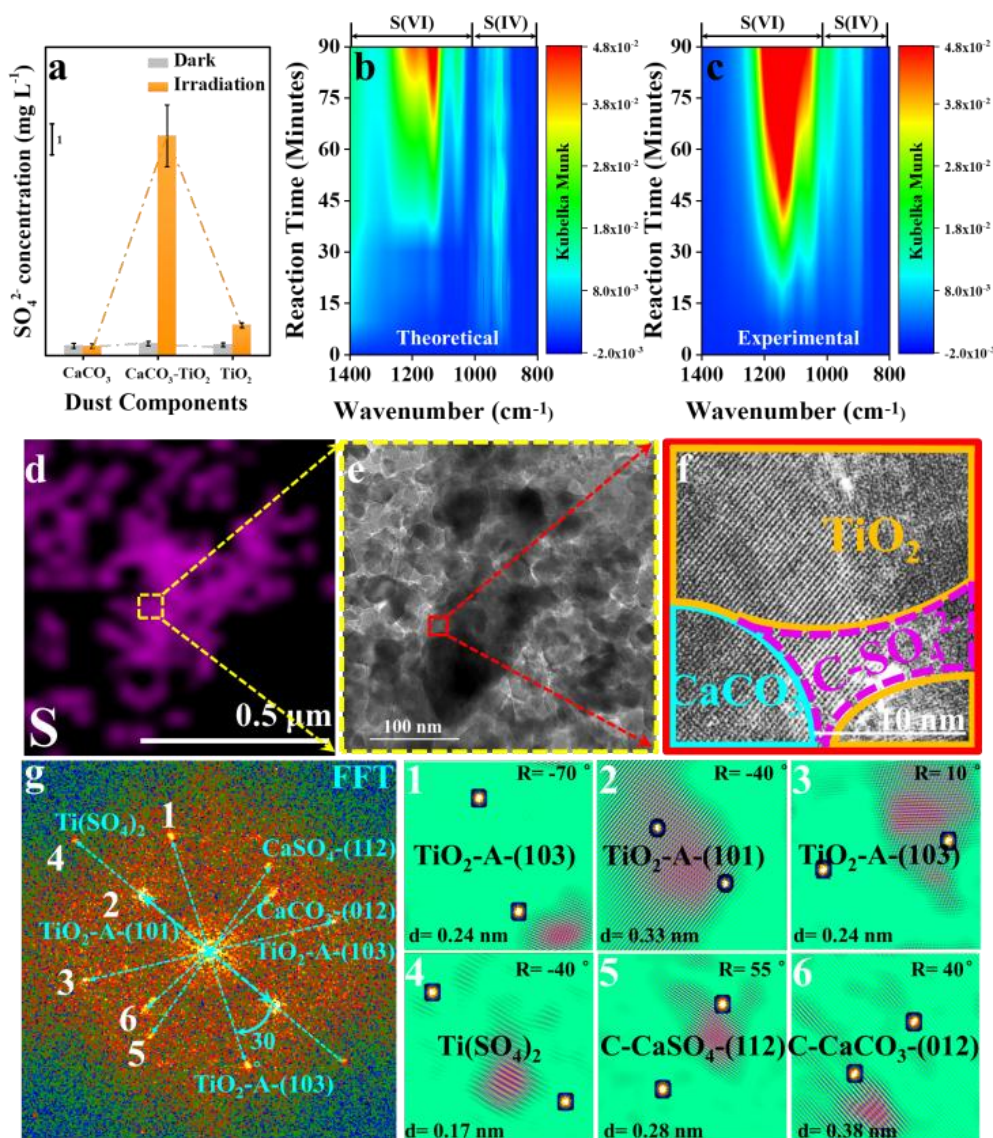
3.2.1 Accelerated sulfate production in the presence of carbonate.

The phy-chemical properties of employed mineral dust proxies were first characterized (Fig. S1), consistent with earlier reported studies (Su et al., 2008; Balachandran and Eror, 1982; Shang et al., 2010), and spectral irradiance of the solar simulator applied in the present study is well covered by natural sunlight (Fig. S2), as much as possible having experimental results from the lab better applicability in the real atmosphere. The sulfate yield, measured by IC, upon irradiation on TiO₂-CaCO₃ mixture particles (50 wt. % CaCO₃) is significantly enhanced by 7 times and 23 times compared to that of pristine TiO₂ and CaCO₃ (Fig. 1a), respectively. In stark contrast, there is a negligible increase of sulfate production detected on the TiO₂-CaCO₃ mixture relative to that of pristine CaCO₃ and TiO₂ in dark experiments (Fig. 1a). This result allows us to consider that in addition to alkaline environment alternative important force resulting in the remarkable increase of sulfate yield upon irradiation is expected within the carbonate-containing system. Fig. 1b and 1c show the *in situ* diffuse reflectance infrared DRIFTS features of S(IV) and S(VI) species formed on theoretical and experimental TiO₂-CaCO₃ mixtures (wt./wt. = 50/50) upon irradiation for 90 min, respectively. The “theoretical” here is calculated based on the *in situ* DRIFTS of pristine TiO₂ and CaCO₃ through a simple linear superposition. These results suggest a synergistic effect presented in this mixture for sulfate formation under solar irradiation. In addition, a more evident fingerprint SO₄²⁻ feature (Dong et al., 2009; Yann Batonneau et al., 2008) monitored by Raman spectroscopy appears over TiO₂-CaCO₃ particles compared to pristine TiO₂ particles (Fig. S3), in good agreement with the IC analyses and *in situ* DRIFTS measurements. Combining DRIFTS experiments with the obtained calibration curve (Fig. S4), we estimated that the uptake coefficient of TiO₂-CaCO₃ mixture (50 wt. % CaCO₃) is increased by about 17 times as compared to that of pure CaCO₃ or TiO₂ (Table S3). More importantly, upon irradiation SO₂ uptake coefficients for these dust proxies lie at the order of magnitudes of 10⁻⁴, indicating that the photochemical pathway associated with carbonate species is likely a potential driving force to trigger fast SO₂ oxidation in the atmosphere.

High-resolution transmission electron microscopy (HRTEM) analysis of TiO₂-CaCO₃ particles after reaction, in combination with energy dispersive spectrometer mapping measurements of sulfur component, were conducted to investigate the synergistic effect between TiO₂ and carbonate ions (Fig. 1 d-f and Fig. S5). A region with a relatively high density of sulfur species was selected for further observation and the distribution of each component (Fig. 1g) was determined by fast Fourier transformation (FFT) and inverse FFT analyses of the selected HRTEM image in high resolution with lattice fringes shown in Fig. 1f. Observation of crystalline Ti(SO₄)₂ and CaSO₄ on the interface of TiO₂ and CaCO₃ components imply that the synergistic effect on sulfate production likely originates from interplays of those two types of components under solar illumination. We further assessed the importance of interfacial contact between TiO₂ and CaCO₃ in sulfate production by two synthesis approaches in which the interface abundance is modulated for comparison. Typically, a “grinding” method was used to make TiO₂-CaCO₃ mixture with tight contact between those two components, thus leading to a strong interaction. Meanwhile, the “shaking” method is designed to create a TiO₂-CaCO₃ mixture with weak interplay,



leaving relatively fewer amounts interfaces within the mixtures. Indeed, the resulting mixing statuses of two samples meet our expectations, evidenced by the scanning electron microscope (SEM) technique (Fig. S6). IC quantification analysis suggests that particles with considerable junctions exhibit a more pronounced promotion for sulfate yield than those having relatively few junctions (Fig. S7). These results emphasize the importance of an indispensable interface connection between TiO₂ and CaCO₃ in fast production upon irradiation.



130 **Figure 1.** (a) Sulfate concentration quantified by IC on mineral dust particles after exposure to gaseous SO₂ under irradiation or dark for 30 min. *In situ* DRIFTS of S(IV) and S(VI) species yield on theoretical (b) and (c) experimental TiO₂-CaCO₃ mixtures (wt./wt. = 50/50) upon irradiation for 90 min. Reaction conditions: RH = 30 %, Light intensity (I) = 30 mW cm⁻², Total flow rate = 52.5 mL min⁻¹ and SO₂ = 2.21 × 10¹⁴ molecules cm⁻³. All spectra were processed by the Kubelka-Munk (K-M) algorithm. Noting that the production of sulfur species in theoretical TiO₂-CaCO₃ mixtures refer to 0.5 × K-M bands of sulfur species of TiO₂ + 0.5 × K-M bands of sulfur species of CaCO₃



135 while that for experimental TiO₂-CaCO₃ mixtures refer to 1 × K-M bands of sulfur species of TiO₂-CaCO₃ mixtures (wt./wt. = 50/50). **(d)**
Energy Dispersive Spectroscopy (EDS) mapping of sulfur. **(e)** Selected HRTEM region containing a high density of sulfur for further
observation and the red rectangle refers to the region shown in panel f. **(f)** The HRTEM image in high resolution with lattice fringes and **(g)**
corresponding FFT power spectra, lattice indexing, and (1-6) inverse FFT analysis of lattice signal shown in panel g. In panel f, the term
C-SO₄²⁻ stands for crystalline SO₄²⁻, i.e. CaSO₄ and Ti(SO₄)₂. Particles for the HRTEM measurement refer to TiO₂-CaCO₃ mixture
140 particles upon exposure to the 4.42 × 10¹⁴ molecules cm⁻³ SO₂/N₂+O₂ for 60 min while other reaction conditions are as same as that of
above sulfate quantification experiments.

Except for the consideration of heterogeneous reaction over TiO₂, CaCO₃, and TiO₂-CaCO₃ mixtures, the rapid SO₂
oxidation pathway was further probed by employing mineral dust simulants where two dominant crust constituents SiO₂ and
Al₂O₃ were introduced into TiO₂-CaCO₃ particles to mimic the authentic mineral dust particles in the atmosphere, with
specific component and corresponding ratio information shown in Table S1. It worth mentioning that the determination of
145 the ratio of each component in the simulants relies on the EDS mapping results of ATD particles. In Fig. S8, the introduction
of TiO₂ components (≈ 1 % wt.) into SiO₂-Al₂O₃ leads to 81.6 % enhancement of sulfate production while merely 24.8 %
wt. increase of sulfate yield was observed once ≈ 8 % wt. of CaCO₃ was incorporated into SiO₂-Al₂O₃ dust particles.
Surprisingly, mixing of ≈ 1 % mass fraction of TiO₂ and ≈ 8 % wt. of CaCO₃ into SiO₂-Al₂O₃ gives rise to a 235 %
increase of sulfate formation relative to that of SiO₂-Al₂O₃. Hence, the synergistic effect on heterogeneous oxidation of SO₂
150 is likely to take effect in the atmosphere.

3.2.2 Accelerated sulfate production in the presence of CO₂.

Atmospheric CO₂ is also an important source of (bi)carbonate. Its influence on photochemical SO₂ uptake on mineral dust
was thus studied. In the presence of atmospherically relevant CO₂ (9.83 × 10¹⁵ molecules cm⁻³), sulfate yield was increased
under irradiation as compared to CO₂-free case (Fig. 2a and b). We cautiously check the buffering effect of formed
155 (bi)carbonate on sulfate production by time-resolved DRIFTS spectra (Fig. 2c and d). CO₂ suppresses both S(IV) and S(VI)
products under the dark. Instead of accumulating much more sulfur species through buffering effect, (bi)carbonate ions that
evolve active intermediates upon irradiation may be a plausible force to drive rapid sulfate formation. The reaction kinetics
of SO₂ on mineral dust particles follows the pseudo-first-order, as evidenced by the SO₂ concentration dependence
experiments (Fig. S9 a-f). Besides, a nearly 50 % increase of SO₂ uptake coefficient is observed for the mineral dust proxy
160 TiO₂ after being exposed to 9.83 × 10¹⁵ molecules cm⁻³ (400 ppm) CO₂+SO₂/N₂+O₂ mixture.

As another step toward a real scenario in the atmosphere, experimental trials employing authentic dust particles, i.e.
Arizona test dust (ATD), clays IMt-2 (Illite, Mont., USA) and K-Ga-2 (Kaolin, Georgia, USA), were carried out (Table S2).
In Fig. S10, K-Ga-2 clay exhibits the most remarked promotional effect on sulfate yield (by nearly 120 % increased sulfate
production in the CO₂-involved case under irradiation). This correlates with its considerable TiO₂ contents (3.43 %) in the K-
165 Ga-2 clay, in which active intermediates are readily evolved from TiO₂ and (bi)carbonate species upon irradiation. However,
the promotional effect of CO₂ on sulfate production under irradiation is weak for IMt-2 (the content of TiO₂ ≈ 0.99 %) and
ATD (the content of TiO₂ ≈ 0.46 %) as compared to K-Ga-2 particles. This may correlate to their higher mass fraction of



alkaline earth metal oxide (denoted as A.E.), which enables dust particles to possess a large number of (bi)carbonate species in the natural environment where they have experienced long-term exposure to atmospheric CO₂. Therefore, the
170 aforementioned synergetic effect takes effect over IMt-2 and ATD particles even without exposure to CO₂ due to the presence of abundant formed carbonate, and a less evident increase of sulfate yield is observed.

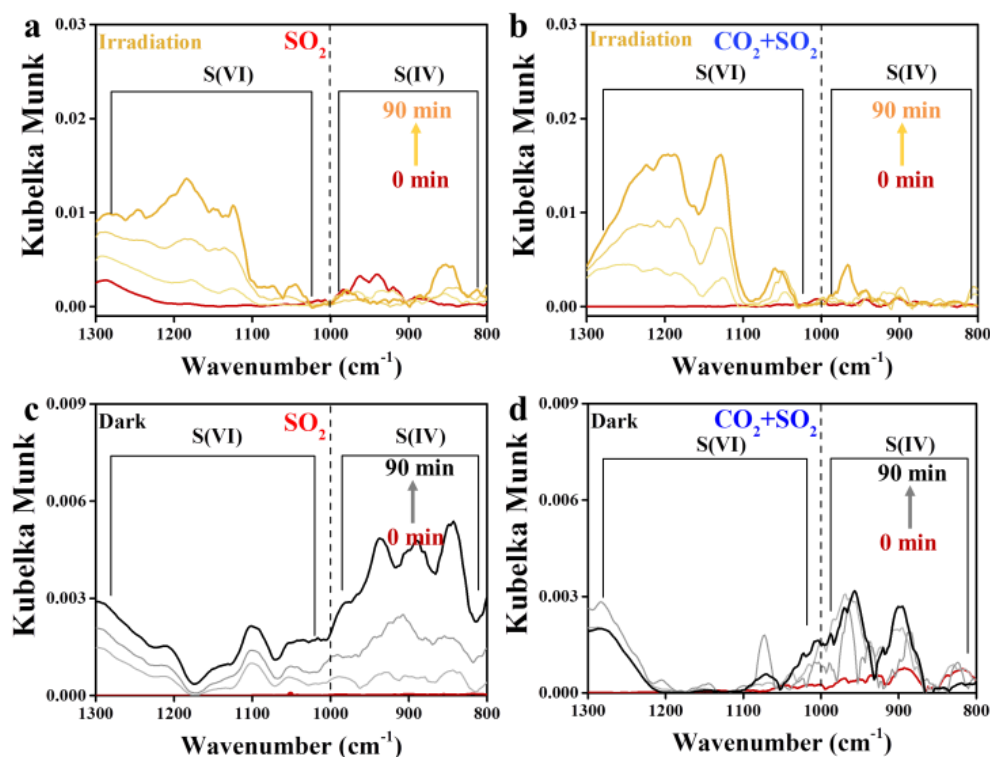


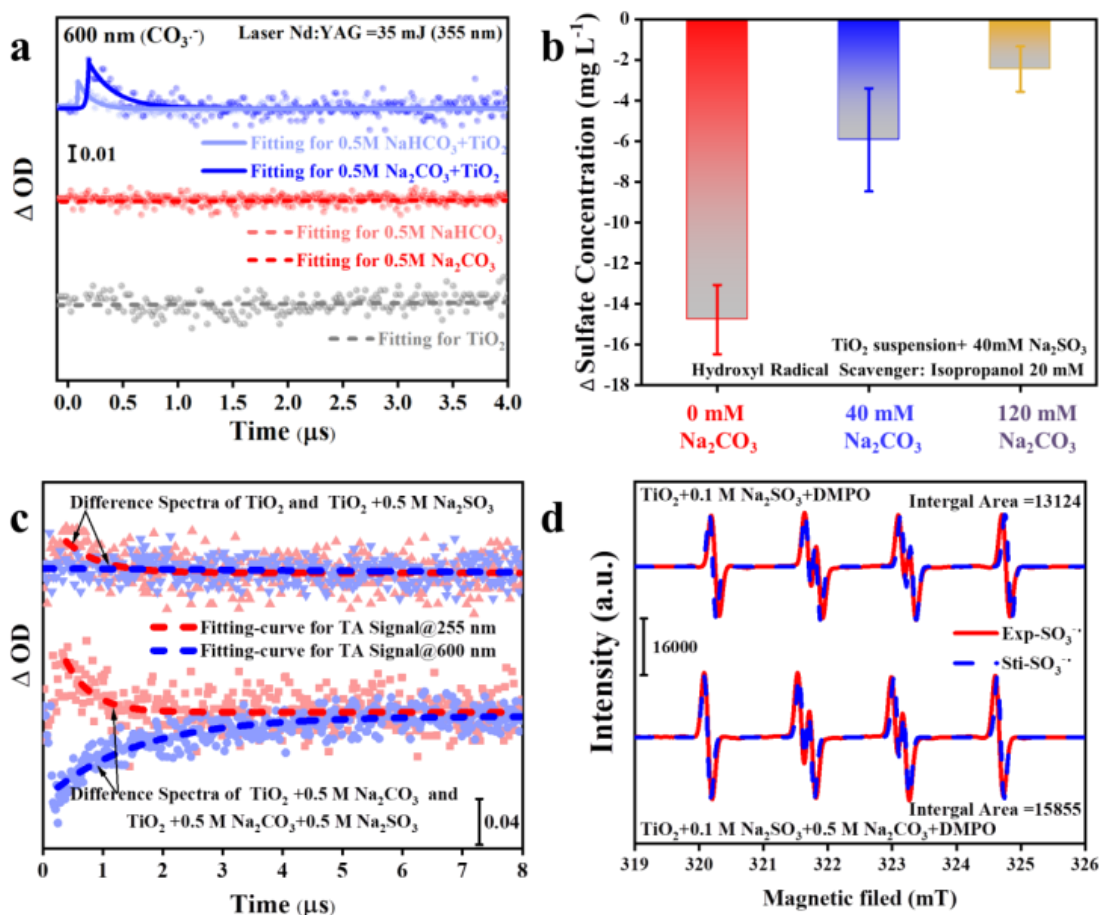
Figure 2. Time-resolved DRIFTS of S(IV) and S(VI) products over TiO₂ particles after exposure to SO₂/N₂+O₂ in the absence and presence of CO₂ upon irradiation (a and b) and those reactions under dark (c and d). Reaction conditions: RH = 30 %, Light intensity (I) =
175 30 mW cm⁻², total flow rate = 52.5 mL min⁻¹ and SO₂ = 7.37 × 10¹³ molecules cm⁻³.

3.2.3 Reaction Mechanism.

The heterogeneous reaction of SO₂ on dust particles in the atmosphere is a complicated process, covering a series of reactions taking place through both homogeneous and heterogeneous ways. Many studies pointed out that dust particles in the atmosphere are more likely to possess several water layers (Vlasenko et al., 2006; Pradhan et al., 2010; Yang et al., 2017)
180 through a thermodynamic equilibrium process, and particles are subjected to provide quasi-aqueous medium when RH is over 20 % (Yu and Jang, 2018). Therefore, the adsorption process mediated by formed water layers can be a major route for gas-dust partitioning, and the aqueous radical-initiated reactions are very likely to responsible for the rapid oxidation of SO₂ on mineral dust surfaces. Earlier sulfate quantification results suggest that intermediates originated from carbonate salt and CO₂ gives rise to fast oxidation of SO₂ on dust particles upon irradiation. In our carbonate-containing reaction system, a
185 plausible intermediate is an active carbonate radical. They are readily produced via the following two pathways. First of all,



carbonate anion can be directly oxidized by produced photo-induced holes (Eqs 2 and 3), as the redox potential of $\text{CO}_3^{\cdot-}/\text{CO}_3^{2-}$ is 1.78 V (vs NHE, at pH = 7), which is lower than the TiO_2 valence band (VB) potential of 2.67 V (vs NHE, at pH = 7) (Li et al., 2016; Xiong et al., 2016):



190 **Figure 3.** (a) Single-wavelength transient absorption spectra of various aqueous solutions. (b) Sulfate formation change $\Delta(\text{SO}_4^{2-})$
 195 determined by different sulfate concentrations with and without the addition of isopropanol as hydroxyl radical scavenger. (c) The
 difference in transient absorption kinetics of sulfite radical and carbonate radical at the various aqueous solutions and their corresponding
 growth-decay fit curves. ΔA -signal was recorded at 255 and 600 nm after pulsed 355 nm laser excitation. (d) ESR spectrometry of
 200 [DMPO- $\text{SO}_3^{\cdot-}$] intermediate formed in a solution of d TiO_2 (3mg~4 mL) + 0.1 M Na_2SO_3 and TiO_2 (3mg~4 mL) + 0.5 M Na_2CO_3 + 0.1 M
 195 Na_2SO_3 . For clarity, the integrated areas of ESR profiles were also presented for direct comparison. Exp. and Sti. stand for experimental
 results and corresponding fitting results using software Isotropic Radicals.



200 In the second pathway, carbonate radicals evolve through the reaction of (bi)carbonate anion with formed hydroxyl radicals
 $\cdot\text{OH}$ over mineral dust surfaces (Zhang et al., 2015a) (Eqs 3 and 4).



The above assumptions are supported by nanosecond transient absorption spectra (NTAS), in which signal (ΔOD) of carbonate radical $CO_3^{\cdot -}$ at 600 nm (Bhattacharya et al., 1998) only emerged for dust suspension containing (bi)carbonate species (Fig. 3a). The $CO_3^{\cdot -}$ -induced chemistry was further evidenced by $\cdot OH$ scavenging experiments using isopropanol as it shows a lower reaction rate with $CO_3^{\cdot -}$ ($K_{i-PrOH-CO_3^{\cdot -}} < 4.0 \times 10^4 \text{ M}^{-1} \text{ s}^{-1}$) relative to that with $\cdot OH$ ($K_{i-PrOH-\cdot OH} < 1.9 \times 10^9 \text{ M}^{-1} \text{ s}^{-1}$) (Buxton et al., 2009; Liu et al., 2015). Clearly, a significant loss of sulfate yield when TiO_2 suspension was added with $\cdot OH$ scavenger (Fig. 3b). However, this is in strong contrast to the result of a carbonate-involved system where the reactivity is sustained, i.e., carbonate radicals offer an alternative reaction pathway for SO_2 oxidation. In addition to laboratory investigations, the carbonate radical formation process is proved to be thermodynamically favorable, supported by density functional theory (DFT) calculations (Fig. S11).

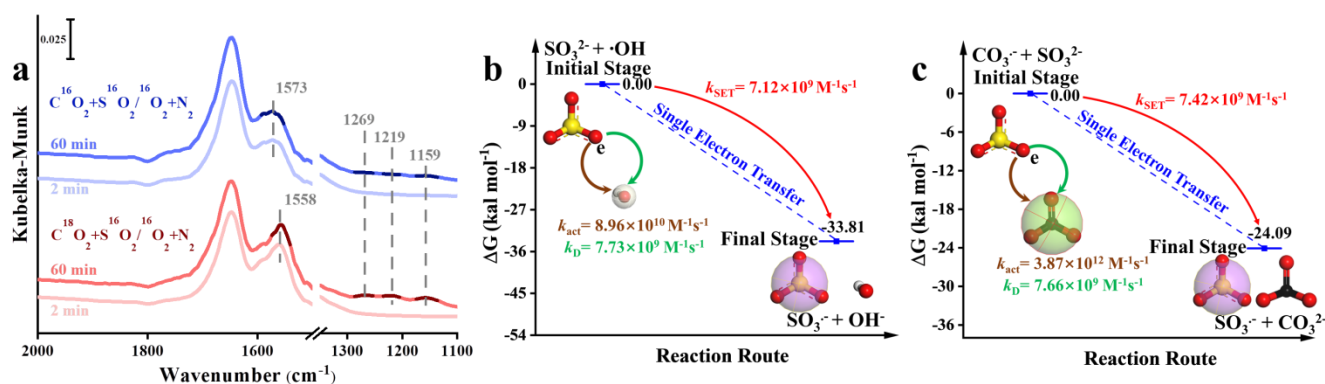


Figure 4. (a) *In situ* DRIFTS of heterogeneous reaction of SO_2 on the TiO_2 particles for 2 and 60 min after being exposed to $C^{16(18)}O_2/N_2$ for 20 min under irradiation. (b) Reaction pathway of interaction between hydroxyl radical ($\cdot OH$) and sulfite (SO_3^{2-}) and (c) Interaction between carbonate radical ($CO_3^{\cdot -}$) and sulfite (SO_3^{2-}) through the SET process at the CCSD (T)-F12/cc-PVDZ-F12//M06-2X/6-311++G (3df, 3pd) level and ΔG_0^{SET} represents the difference in Gibbs free energy between reactant and product. The white, black, yellow, and red spheres represent H, C, S, and O atoms, respectively. In order to guide the attention of the variation of surface products in oxygen isotope experiments (panel a), DRIFTS features of these concerned species were plotted in dark colors.

220

On the other hand, the previous studies (Das, 2001; Neta and Huie, 1985; Chameides and Davis, 1982) agree with the key role of sulfite radical ($SO_3^{\cdot -}$) in rapid sulfate production in an aqueous medium, and the present reaction system creates a localized environment where $SO_3^{\cdot -}$ can be readily stemmed from the TiO_2 and S(IV) species upon solar illumination (Salama et al., 1995). Consequently, probe light of NTAS at wavelength 255 nm (ascribed to sulfite radical) and 600 nm (ascribed to carbonate radical) were simultaneously monitored (Hayon et al., 1972; Ghalei et al., 2016; Goldstein et al., 2001). A weak signal of sulfite radical was observed in the system of $TiO_2 + Na_2SO_3$ suspension under irradiation (Fig. 3c.). On the contrary, the sulfite radical signal is strengthened after the introduction of Na_2CO_3 into the $TiO_2 + Na_2SO_3$ suspension, along



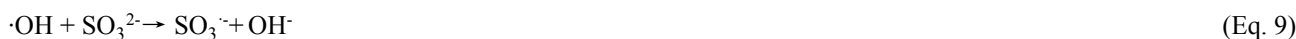
with a significant decrease of signal for carbonate radical. ESR data (Fig. 3d) further confirms the increase of SO_3^- after 2 min UV irradiation in the presence of carbonate ion. Based on the above results, one may deduce that the interplay between carbonate radical and sulfite ions is a crucial step giving rise to the increased SO_3^- which is responsible for rapid SO_2 oxidation through chain propagation reactions (Deng et al., 2017). Nevertheless, there are two possibilities that might explain the aforementioned interaction. One is the oxygen transfer and the other route is electron transfer, which needs further clarification.

We first examined the oxygen transfer path through ^{18}O isotope labeling experiments. TiO_2 particles were initially exposed to $\text{C}^{16}\text{O}_2/\text{N}_2$ and $\text{C}^{18}\text{O}_2/\text{N}_2$, followed by the exposure of $\text{SO}_2/\text{N}_2+\text{O}_2$ under irradiation (Fig. 4a). Bidentate carbonate band centered at 1573 cm^{-1} appears after the introduction of $\text{C}^{16}\text{O}_2/\text{N}_2$, while this band shifts to 1558 cm^{-1} when $\text{C}^{18}\text{O}_2/\text{N}_2$ is introduced, indicating the incorporation of ^{18}O into bidentate carbonate species, in good agreement with the previous report (Liao et al., 2002). However, none shift of IR features at $1269, 1219, \text{ and } 1159\text{ cm}^{-1}$, assigned to (bi)sulfate species on TiO_2 particles, were observed throughout the reaction. This implies that the oxygen transfer path does not account for the rapid SO_2 oxidation on particles of concern.

In light of the above analysis, the electron transfer might be a plausible pathway to explain the fast oxidation within the reaction system. DFT calculations provide an accessible approach to study the electron transfer pathway. The result in Fig. 4b shows SO_3^- formation is a SET process of CO_3^- and SO_3^{2-} , where O atom in SO_3^{2-} transfers an electron to O atom in CO_3^- to form SO_3^- and CO_3^{2-} . This SET reaction is a thermodynamically favorable process, with the difference of Gibbs free energy between reactant and product lying at $-24.09\text{ kcal mol}^{-1}$. Taken above results and discussions together, the following reactions are proposed accordingly (Eqs. 5-8):



Another important issue needs to be addressed as well. We noted that SO_3^- can also be formed via the conventional reaction of $\cdot\text{OH}$ and SO_3^{2-} (Eqs. 9) and this process is also considered.



In this SET process, electron donor SO_3^{2-} reacts spontaneously with electron acceptor $\cdot\text{OH}$ (Fig. 4c) and the calculated activation free energy barrier $\Delta G_{\text{SET}}^\ddagger$ for this SET reaction is $2.50\text{ kcal mol}^{-1}$. Hence, the reaction process of $\cdot\text{OH}$ with SO_3^{2-} is diffusion-controlled, and the total rate constant $k_{\text{SET-2}}$ was calculated to be $7.12 \times 10^9\text{ M}^{-1}\text{s}^{-1}$. In comparison, the rate constant $k_{\text{SET-1}}$ of the diffusion-controlled SET process for CO_3^- and SO_3^{2-} was estimated to be $7.42 \times 10^9\text{ M}^{-1}\text{s}^{-1}$. Despite a slight net increase of the rate, the distinguishable concentration of CO_3^- and $\cdot\text{OH}$ should also be taken into account for the rate comparison in varied reaction paths. To visualize the difference, relative rates were calculated according to Eq. 10:



$$r = \frac{v_{\text{CO}_3^{\cdot-} + \text{SO}_3^{2-}}}{v_{\cdot\text{OH} + \text{SO}_3^{2-}}} = \frac{k_{\text{SET-1}}[\text{CO}_3^{\cdot-}][\text{SO}_3^{2-}]}{k_{\text{SET-2}}[\cdot\text{OH}][\text{SO}_3^{2-}]} \quad (\text{Eq.10})$$

Where r is the ratio of two reaction rates, $[\text{CO}_3^{\cdot-}]$, $[\text{SO}_3^{2-}]$, and $[\cdot\text{OH}]$ refer to the concentration of corresponding reactants. Previous literature suggests the concentration of carbonate radicals is able to show two orders of magnitude higher than that of hydroxyl radical at the surface of the water under solar irradiation (Chandrasekaran and Thomas, 1983; Goldstein et al., 2001; Shafirovich et al., 2001). Aqueous medium that attach to particle surfaces offer an ideal environment for accumulating carbonate radicals. Consequently, concentrations of $\text{CO}_3^{\cdot-}$ and $\cdot\text{OH}$ were set at the range from 1.0×10^{-10} to 1×10^{-12} mol L⁻¹ and from 1.0×10^{-12} to 1×10^{-14} mol L⁻¹ (Sulzberger et al., 1997b) and r value could thus reach to 1.04×10^4 at most (Fig. S12). As a result, we speculate that the formation pathway of $\text{SO}_3^{\cdot-}$ via interaction between $\text{CO}_3^{\cdot-}$ and SO_3^{2-} is a more effective route, corresponding well with experimental results.

3.2.4 Field Measurements of Sulfate and (Bi)carbonate Ions.

Complement field sampling and analysis provide indirect evidence to support our hypothesis that intermediates $\text{CO}_3^{\cdot-}$ may affect sulfate formation in the atmosphere. Previously, it has been suggested that coarse-model particulate matter (PM) possesses a large mass fraction of mineral dust (Fang et al., 2017; Miller-Schulze et al., 2015), in which TiO_2 was found at mass mixing ratios ranging from 0.1 to 10 % depending on the exact location where particles were uplifted (Hanisch and Crowley, 2003). In this case, PM with relatively larger size dimensions is expected to contribute to secondary sulfate formation via heterogeneous reactions, which is supported by the recent field study where carbonate fraction of coarse PM is evidenced to promote secondary sulfate production (Song et al., 2018). Therefore, rather than determine the concentration of water-soluble ions in all stages, more attention was paid to PM collected in stages 1-4 (particles with their dimension ≥ 3.3 μm). (Bi)carbonate ions are known as key precursors in producing $\text{CO}_3^{\cdot-}$ and accelerate sulfate formation. Quantifications of those relevant species were thus conducted (supplement texts 17 and 18). We further considered the relationships between sulfate ions and (bi)carbonate ions by means of linear regression analysis. In Fig. 5, the negative correlations between the mass concentrations of sulfate ions and (bi)carbonate ions are observed in the nighttime hours, consistent with the suppression of sulfate formation by CO_2 in the dark experiments. This is also supported by our previous study where CO_2 -derived (bi)carbonate species are demonstrated to block the active sites for yielding sulfate over mineral dust proxy aluminum oxide (Liu et al., 2020). Instead, positive correlations are seen for those ions within PM sampled during the daytime hours regardless of size ranges and carbonate types ($\text{HCO}_3^-/\text{CO}_3^{2-}$). Except for the case (nighttime period, size larger than 9 μm), most of the significance P values for their correlations were smaller than 0.1, indicating those correlations do exist for sulfate and (bi)carbonate ions. This matches with the scenarios in which sulfate production upon irradiation in the presence of (bi) carbonate ions are increased over both model and authentic dust particles. In fact, preceding field observations of highly correlated relationship between Ca^{2+} and SO_4^{2-} water-soluble ions (Liu et al., 2020) during the carbonate-enriched dust storm episodes, together with persistent reports on the significant role of photochemical channels in



increasing the sulfate concentration during the daytime (Wei et al., 2019; Kim et al., 2017; Wu et al., 2017) indirectly reflects the possibility of accelerated SO₂ oxidation triggered by photo-response active intermediates related to carbonate species. While we note that the correlation coefficients between sulfate and (bi)carbonate are not high in this work, field measurements of sulfate and (bi)carbonate ions shed light on their distinct correlations during the daytime and nighttime hours. This is the first time that relationships between those ions are explored separately in these two periods. Taken together, carbonate radical is likely to impact the sulfate formation in the atmosphere during the daytime hours.

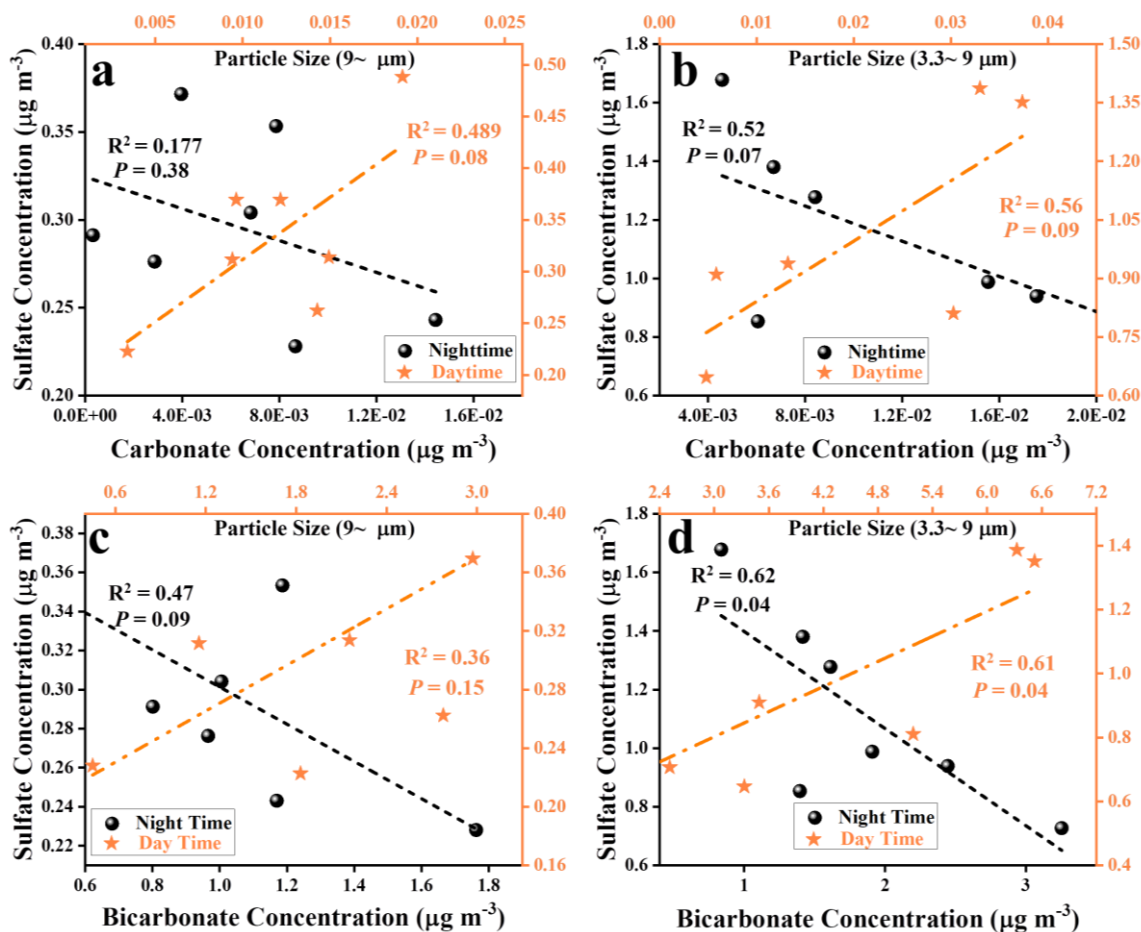


Figure 5. Field observation for the relationship between carbonate and sulfate ions during daytime and nighttime. Linear relationship analyses for measured sulfate ions and estimated carbonate ions (a and b) and for measured sulfate ions and estimated bicarbonate ions (c and d) during the daytime and nighttime at the varied range of particle size 9 μm~ and 3.3~ 9 μm, respectively.



4. Conclusion

Overall, a reaction mechanism for the rapid sulfate formation in the presence of carbonate radicals is summarized and proposed in the scheme (Fig. 6). One may expect that during the nighttime hours CO_2 -derived (bi)carbonate species are prone to have a slightly negative effect on sulfate formation due to the competitive adsorption between CO_2 and SO_2 . On the other hand, both CO_2 -derived carbonate species and carbonate salt works as the precursor of CO_3^- , which largely promotes sulfate formation during the daytime where energetic photons exist. Our observation of strengthened photochemistry launched by carbonate radicals suggests that such chemistry may be amplified on atmospherically relevant reactions over aerosols, where they often contain a large number of hydroxyl radicals and water-soluble (bi)carbonate ions. Since both sulfate aerosol and CO_2 are well known to affect the radiation budget and solar energy balance on the earth, their overall influence on the global climate considering the increased yield of sulfate aerosol triggered by CO_2 , the precursor of carbonate radical, needs further investigation. Therefore, our study highlights the necessity for a comprehensive understanding of the CO_3^- relevant chemistry in the underlying impacts of fine PM concentration, human health, and climate. Moreover, little is known about the interaction between carbonate radicals and other trace gas. Its further influence on the organic aerosol formation also needs consideration since it is known to efficiently participate in some organic compound oxidation reactions. All these assumptions need to be investigated in further detail. This study provides the first indication that carbonate radical not only plays a role as an intermediate in tropospheric anion chemistry but also as a strong oxidant for surfacial processing of trace gas in the atmosphere.

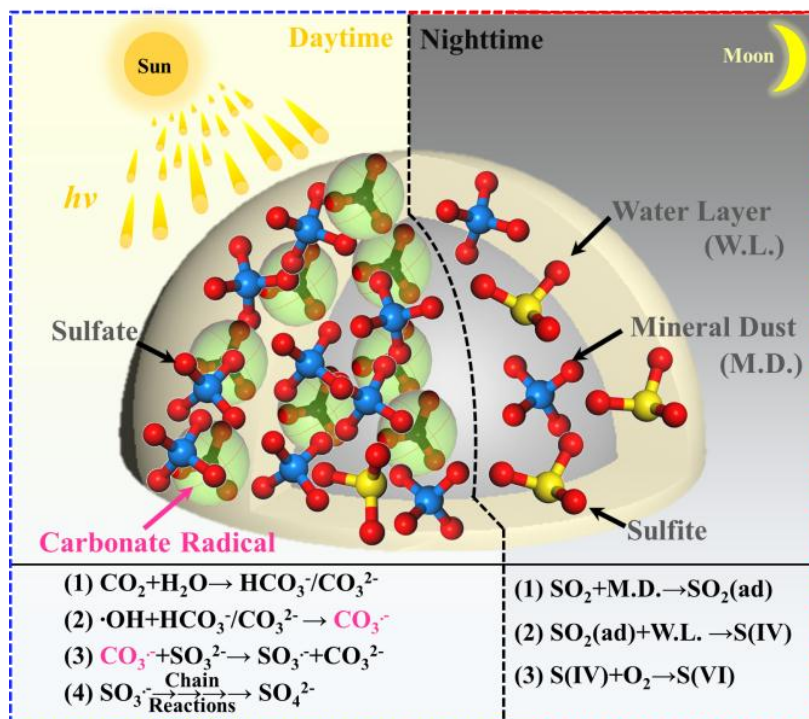


Figure 6. Schematic of the sulfate formation in the presence and absence of carbonate radical.

320

Data availability. The data that support the results are available from the corresponding author upon request.

Author contributions. Y.L., Y.D. and L.Z. initially proposed the idea; Y.L. and Y.D. designed and performed most of the experiments; J.L. performed DFT calculations; Y.L., X.Z. and T.W. contributed to field samplings and data analysis; K.L., K.G., A.B., I.N., X.Z., C.G., and L.Z. provided suggestions on the experiments and paper writing; All authors wrote the manuscript.

325

Competing interests. The authors declare that they have no conflict of interest.

Acknowledgements. We greatly appreciate Dr. Yang Yang and Prof. Keli Han from Dalian institute of chemical physics for NTAS and some helpful discussions.

330

Financial support. This work was supported by the National Natural Science Foundation of China (No. 21976030 and No. 21677037), National key research and development program of China (2016YFE0112200 and 2016YFC0202700), the Natural Science Foundation of Shanghai (No. 19ZR1471200 and No. 17ZR1440200).



335 References

- Balachandran, U., and Eror, N. G.: Raman-Spectra Of Titanium-Dioxide, *J. Solid State Chem.*, 42, 276-282, [https://doi.org/10.1016/0022-4596\(82\)90006-8](https://doi.org/10.1016/0022-4596(82)90006-8), 1982.
- Baltrusaitis, J., Schuttlefield, J., Zeitler, E., and Grassian, V. H.: Carbon dioxide adsorption on oxide nanoparticle surfaces, *Chem. Eng. J.*, 170, 471-481, <https://doi.org/10.1016/j.cej.2010.12.041>, 2011.
- 340 Bao, H., Yu, S., and Tong, D. Q.: Massive volcanic SO₂ oxidation and sulphate aerosol deposition in Cenozoic North America, *Nature*, 465, 909-912, <https://doi.org/10.1038/nature09100>, 2010.
- Beig, G., and Brasseur, G. P.: Model of tropospheric ion composition: A first attempt, *J. Geophys. Res.*, 105, 22671-22684, <https://doi.org/10.1029/2000JD900119>, 2000.
- Bhattacharya, A., Amitabha, D., and Mandal, P. C.: Carbonate radical induced polymerisation of pyrrole: A steady state and flash photolysis study, *J. Radioanal Nucl. Ch.*, 230, 91-95, <https://doi.org/10.1007/BF02387452>, 1998.
- 345 Bisby, R. H., Johnson, S. A., Parker, A. W., and Tavender, S. M.: Time-resolved resonance Raman spectroscopy of the carbonate radical, *J. Chem. Soc. Faraday Trans.*, 94, 2069-2072, <https://doi.org/10.1039/A801239C>, 1998.
- Buxton, G. V., Greenstock, C. L., Helman, W. P., and Ross, A. B.: Critical Review of rate constants for reactions of hydrated electrons, hydrogen atoms and hydroxyl radicals ($\cdot\text{OH}/\text{O}^-$ in aqueous solution, *J. Phys. Chem. Ref. Data*, 17, 513-886, <https://doi.org/10.1063/1.555805>, 2009.
- 350 Cao, J. J., Lee, S. C., Zhang, X. Y., Chow, J. C., An, Z. S., Ho, K. F., Watson, J. G., Fung, K., Wang, Y. Q., and Shen, Z. X.: Characterization of airborne carbonate over a site near Asian dust source regions during spring 2002 and its climatic and environmental significance, *J. Geophys. Res.*, 110, 1-8, <https://doi.org/10.1029/2004JD005244>, 2005.
- Chameides, W. L., and Davis, D. D.: The Free-Radical chemistry of cloud droplets and its impact upon the composition of rain, *Journal of Geophysical Research-Oceans*, 87, 4863-4877, <https://doi.org/10.1029/JC087iC07p04863>, 1982.
- 355 Chandrasekaran, K., and Thomas, J. K.: Photochemical reduction of carbonate to formaldehyde on TiO₂ powder, *Chem. Phys. Lett.*, 99, 7-10, [https://doi.org/10.1016/0009-2614\(83\)80259-0](https://doi.org/10.1016/0009-2614(83)80259-0), 1983.
- Cope, V. W., Chen, S.-N., and Hoffman, M. Z.: Intermediates in the photochemistry of of carbonato-amine complexes of cobalt(III). carbonate(-) radicals and the aquocarbonato complex, *J. Am. Chem. Soc.*, 95, 3116-3121, <https://doi.org/10.1021/ja00791a005>, 1973
- 360 Das, T. N.: Reactivity and role of SO₅- radical in aqueous medium chain oxidation of sulfite to sulfate and atmospheric sulfuric acid generation, *J. Phys. Chem. A*, 105, 9142-9155, <https://doi.org/10.1021/jp011255h>, 2001.
- Davis, A. C., and Francisco, J. S.: Reactivity trends within alkoxy radical reactions responsible for chain branching, *J. Am. Chem. Soc.*, 133, 18208-18219, <https://doi.org/10.1021/ja204806b>, 2011.
- 365 Deng, W., Zhao, H. L., Pan, F. P., Feng, X. H., Jung, B., Abdel-Wahab, A., Batchelor, B., and Li, Y.: Visible-light-driven photocatalytic degradation of organic water pollutants promoted by sulfite addition, *Environ. Sci. Technol.*, 51, 13372-13379, <https://doi.org/10.1021/acs.est.7b06200>, 2017.
- Deng, Y., Liu, Y., Wang, T., Cheng, H., Feng, Y., Yang, Y., and Zhang, L.: Photochemical reaction of CO₂ on atmospheric mineral dusts, *Atmos. Environ.*, 223, 117222.117221-117222.117210, <https://doi.org/10.1016/j.atmosenv.2019.117222>, 2020.
- 370 Dong, J. L., Xiao, H. S., Zhao, L. J., and Zhang, Y. H.: Spatially resolved Raman investigation on phase separations of mixed Na₂SO₄/MgSO₄ droplets, *J. Raman. Spectrosc.*, 40, 338-343, <https://doi.org/10.1002/jrs.2132>, 2009.
- Dotan, I., Davidson, J. A., Streit, G. E., Albritton, D. L., and Fehsenfeld, F. C.: A study of the reaction $\text{O}^{-3} + \text{CO}_2 \sim \text{CO}^{-3} + \text{O}_2$ and its implication on the thermochemistry of CO₃ and O₃ and their negative ions, *J. Chem. Phys.*, 67, 2874-2879, <https://doi.org/10.1063/1.435155>, 1977.
- 375 Fang, T., Guo, H., Zeng, L., Verma, V., Nenes, A., and Weber, R. J.: Highly Acidic Ambient Particles, Soluble Metals, and Oxidative Potential: A Link between Sulfate and Aerosol Toxicity, *Environ. Sci. Technol.*, 51, 2611-2620, <https://doi.org/10.1021/acs.est.6b06151>, 2017.
- Fang, X., Liu, Y., Kejian, Tao, W., Yue, D., Yiqing, F., Yang, Y., Cheng, H., Chen, J., and liwu, Z.: Atmospheric Nitrate Formation through Oxidation by carbonate radical, *ACS Earth Space Chem.*, ASAP, <https://doi.org/10.1021/acsearthspacechem.1c00169>, 2021.
- 380 Ferrer-Sueta, G., Vitturi, D., Batinic-Haberle, I., Fridovich, I., Goldstein, S., Czapski, G., and Radi, R.: Reactions of manganese porphyrins with peroxyxynitrite and carbonate radical anion, *J. Biol. Chem.*, 278, 27432-27438, <https://doi.org/10.1074/jbc.M213302200>, 2003.



- 385 Ghalei, M., Ma, J., Schmidhammer, U., Vandenborre, J., Fattahi, M., and Mostafavi, M.: Picosecond pulse radiolysis of highly concentrated carbonate solutions, *J. Phys. Chem. B*, 120, 2434-2439, <https://doi.org/10.1021/acs.jpcc.5b12405>, 2016.
- Goldstein, S., Czapski, G., Lind, J., and Merényi, G.: Carbonate radical ion is the only observable intermediate in the reaction of peroxyxynitrite with CO₂, *Chem. Res. Toxicol.*, 14, 1273-1276, <https://doi.org/10.1021/tx0100845>, 2001.
- Graedel, T. E., and Weschler, C. J.: Chemistry within aqueous atmospheric aerosols and raindrops, *Reviews of Geophysics*, 19, 505-539, 1981a.
- 390 Graedel, T. E., and Weschler, C. J.: Chemistry within Aqueous Atmospheric Aerosols And Raindrops, *J. Geophys. Res.*, 19, 505-539, <https://doi.org/10.1029/RG019i004p00505>, 1981b.
- Hanisch, F., and Crowley, J. N.: Ozone decomposition on Saharan dust: an experimental investigation, *Atmos. Chem. Phys. Discuss.*, 3, 119-130, <https://doi.org/10.5194/acp-3-119-2003>, 2003.
- Hayon, E., Treinin, A., and Wilf, J.: Electronic spectra, photochemistry, and autoxidation mechanism of the sulfite-bisulfite-pyrosulfite systems. SO₂^{•-}, SO₃^{•-}, SO₄^{•-}, and SO₅^{•-} radicals, *J. Am. Chem. Soc.*, 94, 47-57, <https://doi.org/10.1021/ja00756a009>, 1972.
- Hossain, M. D., Huang, Y., Yu, T. H., Goddard Iii, W. A., and Luo, Z.: Reaction mechanism and kinetics for CO₂ reduction on nickel single atom catalysts from quantum mechanics, *Nat. Commun.*, 11, 2256, <https://doi.org/10.1038/s41467-020-16119-6>, 2020.
- 400 Huang, H. L., Chao, W., and Lin, J. J. M.: Kinetics of a Criegee intermediate that would survive high humidity and may oxidize atmospheric SO₂, *Proc. Natl. Acad. Sci. USA*, 112, 10857-10862, <https://doi.org/10.1073/pnas.1513149112>, 2015.
- Hung, H. M., Hsu, M. N., and Hoffmann, M. R.: Quantification of SO₂ oxidation on interfacial surfaces of acidic microdroplets: Implication for ambient sulfate formation, *Environ. Sci. Technol.*, 52, 9079-9086, <https://doi.org/10.1021/acs.est.8b01391>, 2018.
- 405 Kerminen, V. M., Hillamo, R., Teinilä K., Pakkanen, T., Allegrini, I., and Sparapani, R.: Ion balances of size-resolved tropospheric aerosol samples: implications for the acidity and atmospheric processing of aerosols, *Atmos. Environ.*, 35, 5255-5265, [https://doi.org/10.1016/S1352-2310\(01\)00345-4](https://doi.org/10.1016/S1352-2310(01)00345-4), 2001.
- Kim, H., Zhang, Q., and Heo, J.: Influence of Intense secondary aerosol formation and long range transport on aerosol chemistry and properties in the Seoul Metropolitan Area during spring time Results from KORUS-AQ, *Atmospheric Chemistry and Physics Discussions*, 10.5194/acp-2017-947, 2017.
- 410 Lehtipalo, K., Rondo, L., Kontkanen, J., Schobesberger, S., Jokinen, T., Sarnela, N., Kürten, A., Ehrhart, S., Franchin, A., Nieminen, T., Riccobono, F., Sipilä M., Yli-Juuti, T., Duplissy, J., Adamov, A., Ahlm, L., Almeida, J., Amorim, A., Bianchi, F., Breitenlechner, M., Dommen, J., Downard, A. J., Dunne, E. M., Flagan, R. C., Guida, R., Hakala, J., Hansel, A., Jud, W., Kangasluoma, J., Kerminen, V.-M., Keskinen, H., Kim, J., Kirkby, J., Kupc, A., Kupiainen-Määttä O., Laaksonen, A., Lawler, M. J., Leiminger, M., Mathot, S., Olenius, T., Ortega, I. K., Onnela, A., Petäjä T., Praplan, A., Rissanen, M. P., Ruuskanen, T., Santos, F. D., Schallhart, S., Schnitzhofer, R., Simon, M., Smith, J. N., Tröstl, J., Tsagkogeorgas, G., Tomé A., Vaattovaara, P., Vehkamäki, H., Virtala, A. E., Wagner, P. E., Williamson, C., Wimmer, D., Winkler, P. M., Virtanen, A., Donahue, N. M., Carslaw, K. S., Baltensperger, U., Riipinen, I., Curtius, J., Worsnop, D. R., and Kulmala, M.: The effect of acid-base clustering and ions on the growth of atmospheric nano-particles, *Nat. Commun.*, 7, 11594, <https://doi.org/10.1038/ncomms11594>, 2016.
- 420 Li, X., Yu, J., and Jaroniec, M.: Hierarchical photocatalysts, *Chem. Soc.Rev.*, 45, 2603-2636, <https://doi.org/10.1039/c5cs00838g>, 2016.
- Liao, L. F., Lien, C. F., Shieh, D. L., Chen, M. T., and Lin, J. L.: FTIR study of adsorption and photoassisted oxygen isotopic exchange of carbon monoxide, carbon dioxide, carbonate, and formate on TiO₂, *J. Phys. Chem. B*, 106, 11240-11245, <https://doi.org/10.1021/jp0211988>, 2002.
- 425 Liu, Y., He, X., Duan, X., Fu, Y., and Dionysiou, D. D.: Photochemical degradation of oxytetracycline: Influence of pH and role of carbonate radical, *Chem. Eng. J.*, 276, 113-121, <https://doi.org/10.1016/j.cej.2015.04.048>, 2015.
- Liu, Y., Wang, T., Fang, X., Deng, Y., Cheng, H., Fu, H., and Zhang, L.: Impact of greenhouse gas CO₂ on the heterogeneous reaction of SO₂ on Alpha-Al₂O₃, *Chinese Chem. Lett.*, <https://doi.org/10.1016/j.ccllet.2020.04.037>, 2020.
- 430 McNaughton, C. S., Clarke, A. D., Kapustin, V., Shinozuka, Y., Howell, S. G., Anderson, B. E., Winstead, E., Dibb, J., Scheuer, E., Cohen, R. C., Wooldridge, P., Perring, A., Huey, L. G., Kim, S., Jimenez, J. L., Dunlea, E. J., DeCarlo, P. F., Wennberg, P. O., Crounse, J. D., Weinheimer, A. J., and Flocke, F.: Observations of heterogeneous reactions between Asian



- pollution and mineral dust over the eastern north Pacific during INTEX-B, *Atmos. Chem. Phys.*, 9, 8283-8308, <https://doi.org/10.5194/acpd-9-8469-2009>, 2009.
- 435 Merouani, S., Hamdaoui, O., Saoudi, F., Chiha, M., and Petrier, C.: Influence of bicarbonate and carbonate ions on sonochemical degradation of Rhodamine B in aqueous phase, *J. Hazard Mater.*, 175, 593-599, <https://doi.org/10.1016/j.jhazmat.2009.10.046>, 2010.
- Miller-Schulze, J. P., Shafer, M., Schauer, J. J., Heo, J., Solomon, P. A., Lantz, J., Artamonova, M., Chen, B., Imashev, S., and Sverdlik, L.: Seasonal contribution of mineral dust and other major components to particulate matter at two remote sites in Central Asia, *Atmospheric Environment*, 119, 11-20, 2015.
- 440 Nanayakkara, C. E., Larish, W. A., and Grassian, V. H.: Titanium dioxide nanoparticle surface reactivity with atmospheric gases, CO₂, SO₂, and NO₂: roles of surface hydroxyl groups and adsorbed water in the formation and stability of adsorbed products, *J. Phys. Chem. C*, 118, 23011-23021, <https://doi.org/10.1021/jp504402z>, 2014.
- Neta, P., and Huie, R. E.: Free-radical chemistry of sulfite, *Environ. Health Persp.*, 64, 209-217, <https://doi.org/10.1289/ehp.8564209>, 1985.
- 445 Platt, U., Lebras, G., Poulet, G., Burrows, J. P., and Moortgat, G.: Peroxy radicals from night-time reaction of NO₃ with organic compounds, *Nature*, 348, 147-149, <https://doi.org/10.1038/348147a0>, 1990.
- Pradhan, M., Kyriakou, G., Archibald, A. T., Papageorgiou, A. C., Kalberer, M., and Lambert, R. M.: Heterogeneous uptake of gaseous hydrogen peroxide by Gobi and Saharan dust aerosols: a potential missing sink for H₂O₂ in the troposphere, *Atmos. Chem. Phys.*, 10, 7127-7136, <https://doi.org/10.5194/acp-10-7127-2010>, 2010.
- 450 Prinn, R. G., Huang, J., Weiss, R. F., Cunnold, D. M., Fraser, P. J., Simmonds, P. G., McCulloch, A., Harth, C., Salameh, P., and O'Doherty, S.: Evidence for substantial variations of atmospheric hydroxyl radicals in the past two decades, *Science*, 292, 1882-1888, <https://doi.org/10.1126/science.1058673>, 2001.
- Salama, S. B., Natarajan, C., Nogami, G., and Kennedy, J. H.: The role of reducing agent in oxidation reactions of water on illuminated TiO₂ electrodes, *J. Electrochem. Soc.*, 142, 806-810, <https://doi.org/10.1149/1.2048539>, 1995.
- 455 Shafirovich, V., Dourandin, A., Huang, W., and Geacintov, N. E.: The carbonate radical is a site-selective oxidizing agent of guanine in double-stranded oligonucleotides, *J. Biol. Chem.*, 276, 24621-24626, <https://doi.org/10.1074/jbc.M101131200>, 2001.
- Shang, J., Li, J., and Zhu, T.: Heterogeneous reaction of SO₂ on TiO₂ particles, *Science China-Chemistry*, 53, 2637-2643, <https://doi.org/10.1007/s11426-010-4160-3>, 2010.
- 460 Song, X., Li, J., Shao, L., Zheng, Q., and Zhang, D.: Inorganic ion chemistry of local particulate matter in a populated city of North China at light, medium, and severe pollution levels, *Sci. Total. Environ.*, 650, 566-574, <https://doi.org/10.1016/j.scitotenv.2018.09.033>, 2018.
- Stenman, D., Carlsson, M., Jonsson, M., and Reitberger, T.: Reactivity of the carbonate radical anion towards carbohydrate and lignin model compounds, *J. Wood Chem. Technol.*, 23, 47-69, <https://doi.org/10.1081/Wct-120018615>, 2003.
- 465 Stone, R.: Air pollution. Counting the cost of London's killer smog, *Science*, 298, 2106-2107, <https://doi.org/10.2307/3833025>, 2002.
- Su, H., Cheng, Y., Zheng, G., Wei, C., Mu, Q., Zheng, B., Wang, Z., Zhang, Q., He, K., and Carmichael, G.: Reactive nitrogen chemistry in aerosol water as a source of sulfate during haze events in China, *Sci. Adv.*, 2, e1601530, <https://doi.org/10.1126/sciadv.1601530>, 2016.
- 470 Su, W. G., Zhang, J., Feng, Z. C., Chen, T., Ying, P. L., and Li, C.: Surface phases of TiO₂ nanoparticles studied by UV Raman spectroscopy and FT-IR spectroscopy, *J Phys Chem C*, 112, 7710-7716, <https://doi.org/10.1021/jp7118422>, 2008.
- Sulzberger, B., Canonica, S., Egli, T., Giger, W., Klausen, J., and Gunten, U. v.: Oxidative transformations of contaminants in natural and in technical systems, *Chimia*, 51, 900-907, <https://doi.org/10.1051/epjconf/20101105003>, 1997a.
- 475 Sulzberger, B., Canonica, S., Egli, T., Giger, W., Klausen, J., and von Gunten, U.: Oxidative transformations of contaminants in natural and in technical systems, *Chimia*, 51, 900-907, 1997b.
- Thompson, A. M.: The oxidizing capacity of the earth's atmosphere: probable past and future changes, *Science*, 256, 1157-1165, <https://doi.org/10.1126/science.256.5060.1157>, 1992.
- 480 Vlasenko, A., Sjogren, S., Weingartner, E., Stemmler, K., Gaggeler, H. W., and Ammann, M.: Effect of humidity on nitric acid uptake to mineral dust aerosol particles, *Atmos. Chem. Phys.*, 6, 2147-2160, <https://doi.org/10.5194/acpd-5-11821-2005>, 2006.



- Wang, Y., Wan, Q., Meng, W., and Liao, F.: Long-term impacts of aerosols on precipitation and lightning over the Pearl River Delta megacity area in China, *Atmos. Chem. Phys.*, 11, 12421-12436, <https://doi.org/10.5194/acp-11-12421-2011>, 2011.
- 485 Wei, J., Yu, H., Wang, Y., and Verma, V.: Complexation of Iron and Copper in Ambient Particulate Matter and Its Effect on the Oxidative Potential Measured in a Surrogate Lung Fluid, *Environ Sci Technol*, 53, 1661-1671, 2019.
- Wu, D., Fan, Z., Ge, X., Meng, Y., Xia, J., Liu, G., and Li, F.: Chemical and Light Extinction Characteristics of Atmospheric Aerosols in Suburban Nanjing, China, *Atmosphere*, 8, 149, 2017.
- 490 Xiong, X. Q., Zhang, X., and Xu, Y. M.: Incorporative effect of Pt and Na₂CO₃ on TiO₂-photocatalyzed degradation of phenol in water, *J. Phys. Chem. C*, 120, 25689-25696, <https://doi.org/10.1021/acs.jpcc.6b07951>, 2016.
- Yan, S. W., Liu, Y. J., Lian, L. S., Li, R., Ma, J. Z., Zhou, H. X., and Song, W. H.: Photochemical formation of carbonate radical and its reaction with dissolved organic matters, *Water Res.*, 161, 288-296, <https://doi.org/10.1016/j.watres.2019.06.002>, 2019.
- 495 Yang, W. W., Zhang, J. H., Ma, Q. X., Zhao, Y., Liu, Y. C., and He, H.: Heterogeneous reaction of SO₂ on manganese oxides: the effect of crystal structure and relative humidity, *Sci. Rep.*, 7, 4550, <https://doi.org/10.1038/s41598-017-04551-6>, 2017.
- Yann Batonneau, Sophie Sobanska, Jacky Laureyns, and Bremard, C.: Confocal microprobe Raman imaging of urban tropospheric aerosol particles, *Environ. Sci. Technol.*, 40, 1300-1306, <https://doi.org/10.1021/es051294x>, 2008.
- 500 Yu, T., Zhao, D., Song, X., and Zhu, T.: NO₂-initiated multiphase oxidation of SO₂ by O₂ on CaCO₃ particles, *Atmos. Chem. Phys.*, 18, 6679-6689, <https://doi.org/10.5194/acp-18-6679-2018>, 2018.
- Yu, Z. C., and Jang, M.: Simulation of heterogeneous photooxidation of SO₂ and NO_x in the presence of Gobi Desert dust particles under ambient sunlight, *Atmos. Chem. Phys.*, 18, 14609-14622, <https://doi.org/10.5194/acp-18-14609-2018>, 2018.
- Zhang, G. S., He, X. X., Nadagouda, M. N., O'Shea, K. E., and Dionysiou, D. D.: The effect of basic pH and carbonate ion on the mechanism of photocatalytic destruction of cylindrospermopsin, *Water Res.*, 73, 353-361, <https://doi.org/10.1016/j.watres.2015.01.011>, 2015a.
- 505 Zhang, R., Wang, G., Song, G., Zamora, M. L., Qi, Y., Yun, L., Wang, W., Min, H., and Yuan, W.: Formation of urban fine particulate matter, *Chemical Reviews*, 115, 3803-3855, <https://doi.org/10.1021/acs.chemrev.5b00067>, 2015b.
- Zheng, B., Zhang, Q., Zhang, Y., He, K. B., Wang, K., Zheng, G. J., Duan, F. K., Ma, Y. L., and Kimoto, T.: Heterogeneous chemistry: a mechanism missing in current models to explain secondary inorganic aerosol formation during the January 2013
- 510 haze episode in north China, *Atmos. Chem. Phys.*, 15, 2031-2049, <https://doi.org/10.5194/acp-15-2031-2015>, 2015.